Available online at www.sciencedirect.com
SCIENCE DIRECT®
Journal of Chromatography A, 1006 (2003) 15–31
JOURNAL OF CHROMATOGRAPHY A
www.elsevier.com/locate/chroma

Optimization of simulated moving bed and Vari*col* processes

A. Toumi[a,*], S. Engell[a], O. Ludemann-Hombourger[b], R.M. Nicoud[b], M. Bailly[c]

[a]*Laboratory of Process Control, Universität Dortmund, Emil-Figge-Strasse 70, D-44221 Dortmund, Germany*
[b]*NovaSep sas, Site Eiffel, Boulevard de la Moselle, F-54340 Pompey, France*
[c]*Laboratoire des Sciences du Génie Chimique, 1 Rue Grandville, B.P. 451, F-54001 Nancy, France*

Abstract

A new continuous chromatographic process (Vari*col*) has been presented recently. Its basic principle consists, in contrast to the traditional simulated moving bed (SMB) technology, of an *asynchronous* shift of the inlet/outlet lines in a multi-column system with a recycle loop. Due to the stronger influence of the discrete dynamics on the plant behavior, the design of a Vari*col* process requires the use of model-based optimization to take advantage of the very high flexibility of this process. The equilibrium theory which has been successfully applied to SMB by many practitioners fails to predict the region of complete separation accurately. In this paper, we present a rigorous model-based optimization framework, which can handle the SMB and the novel Vari*col* process in a systematic manner. The feasibility of the approach is demonstrated by the separation of a mixture of propranolol isomers which exhibits a highly non-linear multi-component adsorption behavior. Experimental results are presented and discussed.
© 2003 Elsevier B.V. All rights reserved.

Keywords: Simulated moving bed chromatography; Mathematical modelling; Vari*col* process; Preparative chromatography; Optimization; Propranolol

1. Introduction

Preparative chromatography is attracting more and more interest from the fine chemical and pharmaceutical industry [1–3], both for product development and commercial production. Preparative chromatographic processes can be classified into two categories: discontinuous (batch) or continuous operating modes. Even though the batch or elution chromatography mode has found the largest number of applications up to now [1], simulated moving bed (SMB) chromatography as a continuous process is gaining more and more attention due to its advantages in terms of productivity and eluent consumption [2,4]. Most applications of the SMB process are developed with liquid mobile phases, but also extensions to the gas phase as well as to supercritical liquids were reported [5–8]. Both cases are of great importance to industry and academic research, since the separated mixture is solvent-free, which avoids further post-processing operations.

Vari*col* is a new multi-column continuous process that has been described recently [9,10]. It can be operated in all fields where SMB is employed. Both the SMB and the Vari*col* process consist of a number of columns connected in series with inlet/outlet ports between the columns. In the SMB process, all inlet/outlet lines are shifted simultaneously. In contrast, these lines are shifted asynchronously in the case of

*Corresponding author. Tel.: +49-231-755-5173; fax: +49-231-755-5129.
E-mail address: a.toumi@ct.uni-dortmund.de (A. Toumi).

0021-9673/03/$ – see front matter © 2003 Elsevier B.V. All rights reserved.
doi:10.1016/S0021-9673(03)00430-8

the Varic*ol* process. Thus, the Varic*ol* process offers additional degrees of freedom, the subintervals after which the different ports are moved relative to the main period. By suitable choice of these subintervals the *average* number of columns in the different zones of the Varic*ol* process during one period can be influenced; in contrast to the SMB process, they are rational numbers. The introduction of these parameters simplifies the process description [10,11]. The additional flexibility of the Varic*ol* process can be used to optimize the column distribution among the different zones. This explains the higher efficiency in terms of separated product per amount of solid-phase compared to an SMB process. This was demonstrated in two theoretical case studies consisting of a sugar-mixture with a linear adsorption isotherm and a mixture of amino isomers with a strongly non-linear adsorption behavior [11]. In this work, the definition of the Varic*ol* process was restricted to a subset of the possible configurations, so that at least two optimization runs were needed in order to explore the whole search space.

In order to remove this restriction, a new definition of the optimization variables of the Varic*ol* process was introduced in [12]. It consists of a recursive scheme for the calculation of the initial column distribution and the normalized switching subintervals from given zone lengths. This optimization strategy was applied to a linear sugar mixture (fructose/glucose) yielding 5% to 30% (depending on the number of columns) more feed throughput compared to an SMB process operated under the same conditions. Moreover, it was found that the smaller the total number of columns, the more efficient is the novel Varic*ol* process in comparison to SMB. This was observed also by Ludemann et al. [13], where the Varic*ol* process was applied to the separation of the SB-553261 racemate. The process design in this study was only partly performed by rigorous optimization.

In this work, we report the first experimental verification of the rigorous optimization strategy developed for the Varic*ol* process. This paper is structured as follows: in the first section, the Varic*ol* process is introduced. The second section describes the models for SMB and Varic*ol* processes, which provides the prerequisite for a rigorous optimization. The optimization strategy is presented thereafter. It was applied experimentally to the separation of a racemic mixture of propranolol, a β-blocker. After model validation, optimization runs were carried out for different numbers of columns. In the 6-column case the determined optimal operating points were tested experimentally. The results are shown and discussed.

2. The principle of the SMB and of the Varic*ol* processes

SMB is a practical way of implementing a counter-current chromatographic process [1,14]. A simplified description of the process is given in Fig. 1. It consists of several chromatographic columns connected in series to build a closed-loop system. A counter-current motion of the solid phase with respect to the liquid phase is simulated by *periodically and simultaneously* moving the inlet and outlet lines by one column in the direction of the liquid flow [15–17]. According to the position of the columns relative to the feed and the draw-off nodes, the process can be divided into four different sections (see Fig. 1), each with a specific role in the separation process:

(i) Zone I between eluent and extract lines: desorption of the more retained component
(ii) Zone II between extract and feed lines: desorption of the less retained component
(iii) Zone III between feed and raffinate lines: adsorption of the more retained component
(iv) Zone IV between raffinate and eluent lines: adsorption of the less retained component.

In the SMB process, the lines are shifted *synchronously* [18,19] and the number of columns in each zone of the process is constant over time, regardless of the location of the inlet/outlet lines. The column configuration of the SMB process can therefore be described by specifying how the columns are distributed among the zones. For example, a configuration of 1/2/2/1 in a 6-column system represents a system where zones I and IV always consist of one column and zones II and III always consist of two columns (see Fig. 1).

The Varic*ol* process is a new multicolumn continuous process described in Fig. 2. This new process is based on an *asynchronous* shift of the inlet/outlet

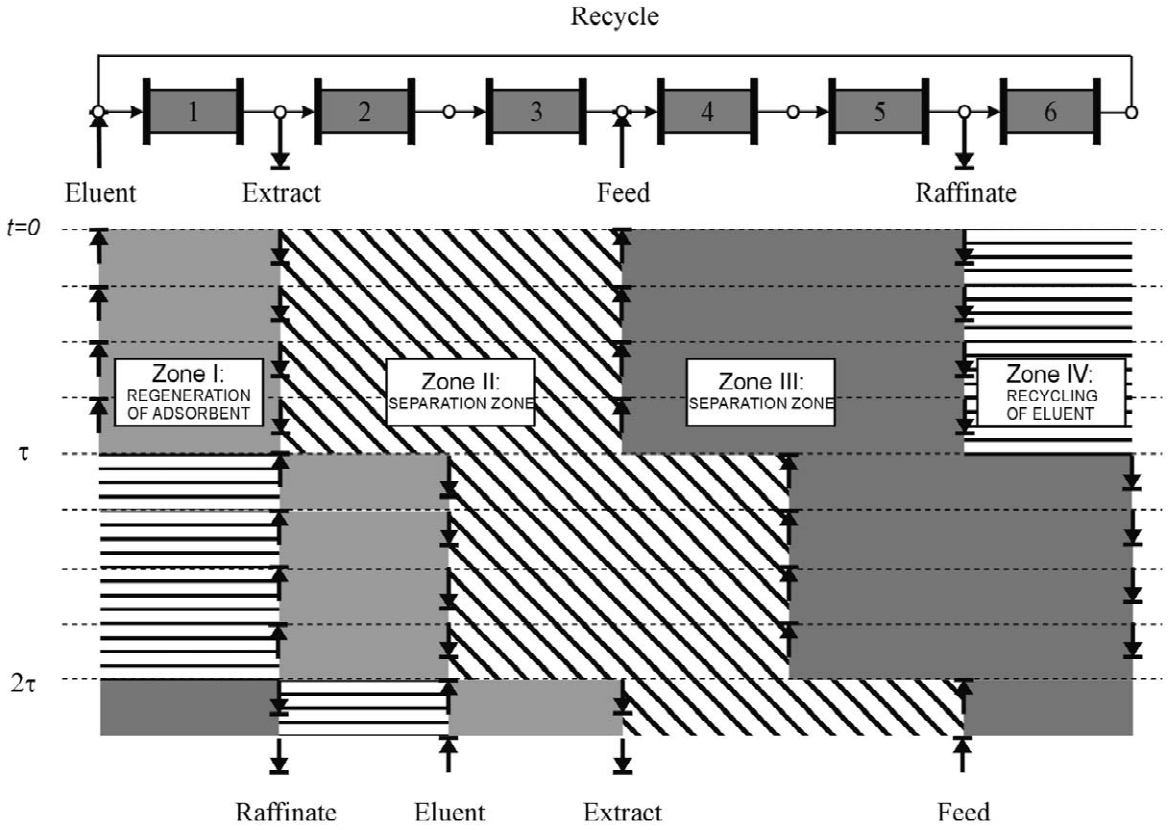

Fig. 1. Chronogram of a 6-column SMB process with column configuration 1/2/2/1.

lines over time (see Fig. 2). Therefore the distribution of the columns between the zones does not remain constant during the period. A compact way to describe the Vari*col* column configuration is to use the average number of columns in each zone of the system. As shown in Fig. 2, the number of columns in zone I is *one* during a quarter of the period and *two* for the rest of the period. This corresponds to an average number of columns of:

$$\overline{N}_1 = 1 \cdot \frac{1}{4} + 2 \cdot \frac{3}{4} = \frac{7}{4} \tag{1}$$

for zone I.

Analogously, for the other zones

$$\overline{N}_2 = \frac{6}{4}, \overline{N}_3 = \frac{9}{4}, \overline{N}_4 = \frac{7}{4}$$

results.

While the SMB process in Fig. 1 has an integer column distribution of (1, 2, 2, 1), the Vari*col* process described in Fig. 2 is characterized by a rational average number of columns in each zone. The sum of the average lengths of the zones must in both cases be equal to the total number of columns:

$$\sum_{i=1}^{4} \overline{N}_i = N_{\text{col,total}} = 6 \tag{2}$$

so that only three of the zone lengths $\overline{N}_1$ can be chosen independently. A Vari*col* process is thus characterized by the total number of chromatographic columns $N_{\text{col,total}}$ used and by three average zone lengths, for example, of the zones I to III, the switching time τ and the different flow-rates.

Unlike a 4-zone SMB process, where for a 4-column system only one configuration is viable (1 column in each zone), in a Vari*col* process, there is a range of possible configurations even in this case.

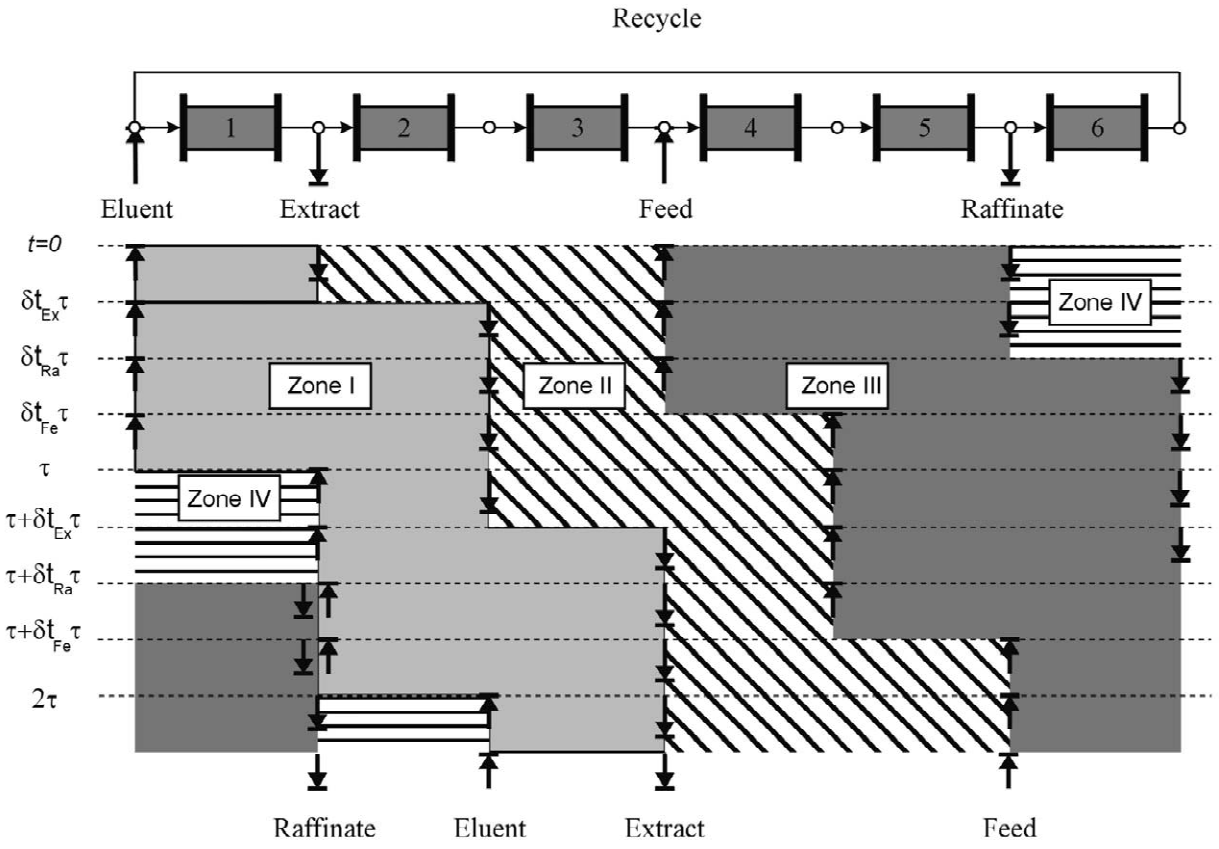

Fig. 2. Chronogram of a 6-column Vari*col* process with average zone lengths of $\frac{7}{4}/\frac{6}{4}/\frac{9}{4}/\frac{2}{4}$.

Thus the Vari*col* process is a promising alternative to SMB when few columns are used.

3. Modeling

A lot of work has been published on the modeling of chromatographic processes [20–22]. Only the most important aspects will be briefly discussed here. Accurate dynamic models of multi-column continuous chromatographic processes consist of dynamic models of each column and the description of the periodic port switching. From mass balances around the inlet and the outlet nodes, the internal fluid velocities of the columns and the product concentrations can be calculated (node model [23]):

$$\begin{aligned}
&\text{Desorbent node} && Q_{\mathrm{IV}} + Q_{\mathrm{De}} = Q_{\mathrm{I}} && \\
&&& c^{\mathrm{out}}_{i,\mathrm{IV}} Q_{\mathrm{IV}} = c^{\mathrm{in}}_{i,\mathrm{I}} Q_{\mathrm{I}} && i = 1, 2 \\
&\text{Extract node} && Q_{\mathrm{I}} - Q_{\mathrm{Ex}} = Q_{\mathrm{II}} && \\
&\text{Feed node} && Q_{\mathrm{II}} + Q_{\mathrm{Fe}} = Q_{\mathrm{III}} && \\
&&& c^{\mathrm{out}}_{i,\mathrm{II}} Q_{\mathrm{II}} + c_{i,\mathrm{Fe}} Q_{\mathrm{Fe}} = c^{\mathrm{in}}_{i,\mathrm{III}} Q_{\mathrm{III}} && i = 1, 2 \\
&\text{Raffinate node} && Q_{\mathrm{III}} - Q_{\mathrm{Ra}} = Q_{\mathrm{IV}} &&
\end{aligned} \tag{3}$$

Here $Q_{\mathrm{I}\ldots\mathrm{IV}}$ denote the internal flow-rates in the corresponding zones, Q_{De}, Q_{Ex}, Q_{Fe} and Q_{Ra} are the external flow-rates and c_i^{out} and c_i^{in} denote the concentrations of the ith component in the stream leaving or entering the respective zone. A single chromatographic column can be described accurately by the *general rate model* [20,22,24] which accounts

for all important non-idealities of the column, i.e. axial dispersion, pore diffusion and the mass transfer between liquid and solid phase. We assume that the solid phase consists of porous, uniform and spherical particles (radius R_p, radial coordinate r) with a void fraction ε_p and that a local equilibrium is established within the pores. The concentration of ith solute component is denoted by c_i in the fluid phase and by q_i in the solid phase. ε_b is the void fraction of the bulk phase, D_{ax} the axial dispersion coefficient, c_i^{eq} the equilibrium concentration, $k_{l,i}$ the film mass transfer resistance and $D_{p,i}$ the diffusion coefficient within the particle pores. The concentration within the pores is denoted by $c_{p,i}$. Then the following set of partial differential equations can be derived from a mass balance around an infinitely small cross-section of the column, if a constant radial distribution of u and c_i is assumed:

$$\begin{aligned}
&\frac{\partial c_i}{\partial t} + \left(\frac{1-\varepsilon_b}{\varepsilon_b}\right)\cdot\frac{3k_{l,i}}{r_p}\left(c_i - c_{p,i|r=r_p}\right) = D_{\mathrm{ax},i}\cdot\frac{\partial^2 c_i}{\partial x^2} - u\cdot\frac{\partial c_i}{\partial x}\\
&(1-\varepsilon_p)\cdot\frac{\partial q_i}{\partial t} + \varepsilon_p\cdot\frac{\partial c_{p,i}}{\partial t} - \varepsilon_p D_{p,i}\left[\frac{1}{r^2}\cdot\frac{\partial}{\partial r}\left(r^2\frac{\partial c_{p,i}}{\partial r}\right)\right]\\
&= 0\\
&q_i = f(c_{p,1},\ldots,c_{p,nsp}) \qquad (4)
\end{aligned}$$

The initial and boundary conditions are

$$\begin{aligned}
&c_{i,t=0} = c_i^{\mathrm{in}};\quad c_{p,i,t=0} = c_{p,i}(0,r,x),\\
&\left.\frac{\partial c_i}{\partial x}\right|_{z=0} = \frac{u}{D_{\mathrm{ax},i}}\cdot\left(c_i - c_i^{\mathrm{in}}\right);\ \left.\frac{\partial c_i}{\partial x}\right|_{z=L} = 0\\
&\left.\frac{\partial c}{\partial r}\right|_{r=0} = 0;\ \left.\frac{\partial c_p}{\partial r}\right|_{r=r_p} = \frac{k_i}{\varepsilon_p D_{p,i}}\cdot\left(c_i - c_{p,i,r=r_p}\right) \qquad (5)
\end{aligned}$$

The adsorption equilibrium has to be determined

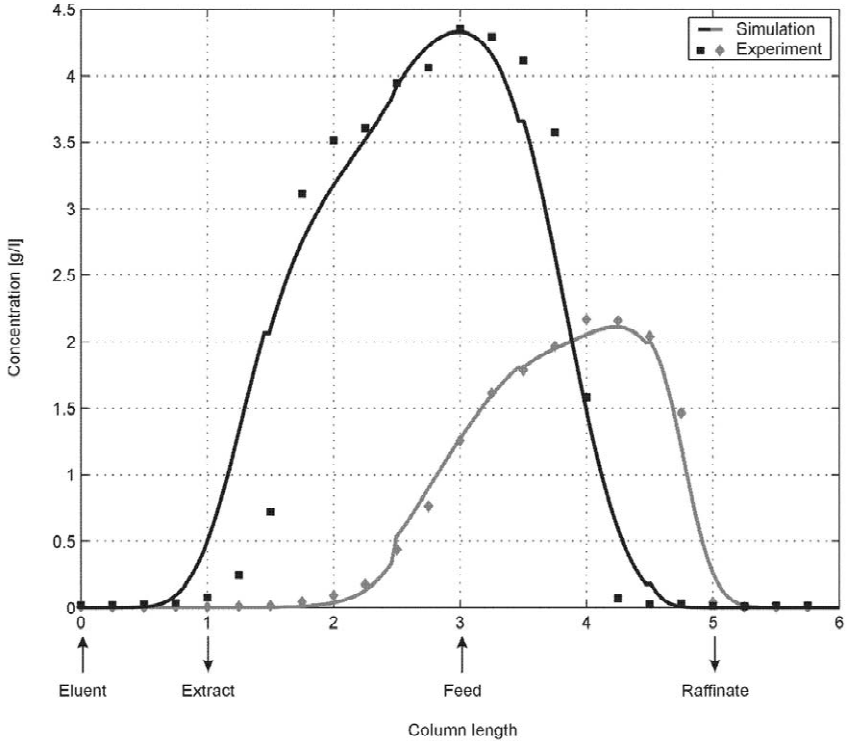

Fig. 3. Comparison of the simulated and experimental axial profiles at the cyclic steady state, 6-column SMB process operated at the conditions listed in column I of Table 1.

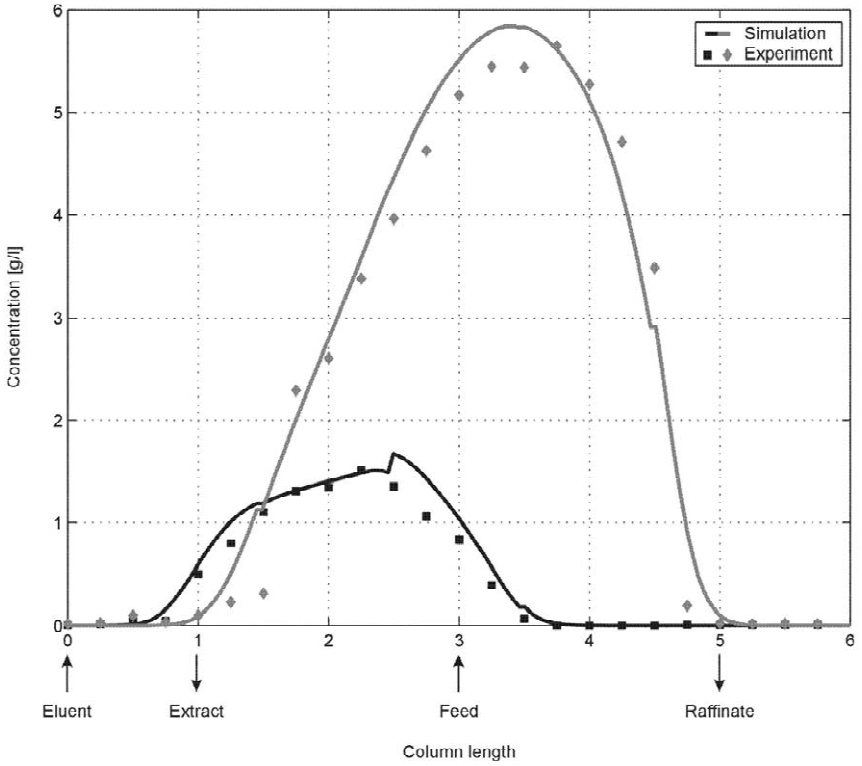

Fig. 4. Comparison of the simulated and experimental axial profiles at the cyclic steady state, 6-column SMB process operated at the conditions listed in column II of Table 1.

experimentally. For the mixture under investigation we obtained a good agreement (see Figs. 3–6) between experimental results and simulation by choosing a modified competitive Langmuir adsorption isotherm:

$$q_i = \lambda_i c_{p,i} + \frac{N k_i c_{p,i}}{1 + \sum_{j=1}^{nsp} k_j c_{p,j}}, \quad i = 1, \ldots, nsp \qquad (6)$$

The resulting system of coupled partial differential equations can be solved efficiently using the numerical technique introduced by Gu [20], where a finite element discretization of the bulk phase is combined with orthogonal collocation of the solid phase. The finite element method with higher order interpolation functions (quadratic functions are used in this work) provides a very powerful method for stiff systems as chromatographic separations, where the concentration gradients in the bulk-fluid phase can be very steep. This method was first applied to SMB processes by Dünnebier et al. [24–26]. The resulting ordinary differential equations can be integrated using an ODE solver such as the package ''lsodi'' developed by Hindmarsh et al. [27], which is based on a modification of Gear's method for stiff ODEs. The *general rate model* can be solved about two orders of magnitude faster than real-time and is the basis of the systematic optimization of operating parameters for both the SMB and the Varic*ol* process discussed below.

4. The optimization strategy

In Klatt et al. [25], the model-based optimization of the operating parameters of continuous chromato-

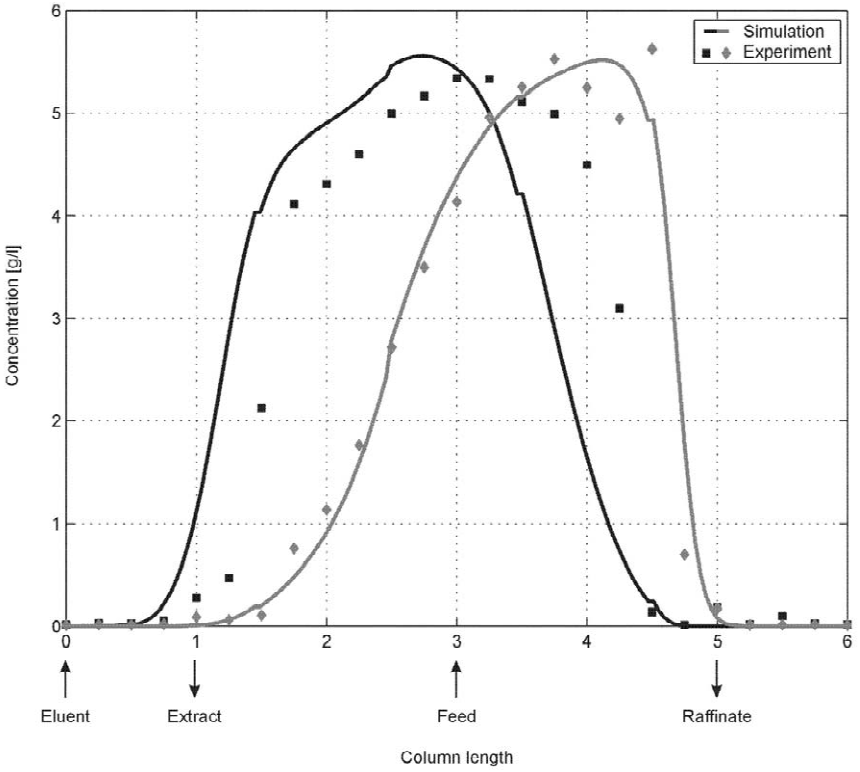

Fig. 5. Optimal cyclic steady state of a 6-column SMB process: comparison of simulation and experiment operated at the conditions listed in column I of Table 2.

graphic processes was introduced in the context of online-control of chromatographic processes. The goal is to find optimal operating parameters for a given separation task on a given plant. The optimization of the distribution of the columns over the zones, i.e. whether the column configuration (1, 2, 2, 1) is better than (2, 1, 2, 1) etc., is a design issue for SMB chromatography and is dealt with in other publications (see e.g. Karlseen et al. [28]). It leads to a complex mixed integer nonlinear program (MINLP). An interesting feature of the Vari*col* process, which will be illustrated in more detail below, is that the choice of the column distribution and the optimization of the operating parameter become closely related issues.

The problem of finding optimal operating parameters for SMB or Vari*col* can be formulated in a similar fashion. The goal is to minimize specific separation costs for a given plant, meeting the required product purities after the process has reached the cyclic steady state (CSS). For the specification of the CSS, the operator Φ is introduced. It represents the process dynamics and the switching operations between two switching intervals. Let $\Phi(c_{\mathrm{ax},k})$ denote the new axial concentration profile relative to the feed port at the end of a switching period, where $c_{\mathrm{ax},k}$ is the concentration profile at the end of the previous period. In the cyclic steady state, the axial concentration profile $c_{\mathrm{ax},k}$ at the end of period k must not change from period to period, i.e.:

$$c_{\mathrm{ax},k+1} - c_{\mathrm{ax},k} = \Phi(c_{\mathrm{ax},k}) - c_{\mathrm{ax},k} = 0 \tag{7}$$

which is checked numerically as

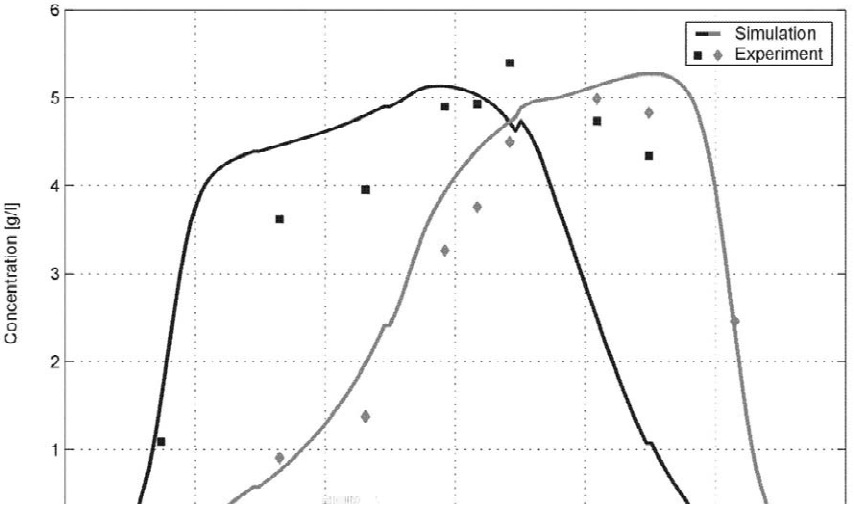

Fig. 6. Optimal cyclic steady state of a 6-column Vari*col* process: comparison of simulation and experiment operated at the conditions listed in column II of Table 2.

$$\|\Phi(c_{\mathrm{ax},k}) - c_{\mathrm{ax},k}\| \leq \varepsilon_{\mathrm{steady}} \tag{8}$$

$\varepsilon_{\mathrm{steady}}$ is a constant (between 10^{-7} and 10^{-6}). Then, given a SMB or Vari*col* process with a total number of columns $N_{\mathrm{col,total}}$, the optimization problem is stated as follows:

$$\begin{aligned} &\min_{\mathbf{u}} Cost_{\mathrm{spec}}(k) \\ &\text{s.t.} \\ &\|\Phi(c_{\mathrm{ax},k}) - c_{\mathrm{ax},k}\| \leq \varepsilon_{\mathrm{steady}} \\ &Pur_{\mathrm{Ex},k} \geq Pur_{\mathrm{Ex,min}} \\ &Pur_{\mathrm{Ra},k} \geq Pur_{\mathrm{Ra,min}} \\ &Q_m \leq Q_{\max} \end{aligned} \tag{9}$$

where the vector **u** of optimization variables in the SMB case consists of the flow-rates of eluent, extract, feed and recycle streams, and the switching period τ. In the Vari*col* case, the three average lengths of the zones $\overline{N}_{\mathrm{I}}$–$\overline{N}_{\mathrm{III}}$ are added to the set of free variables. Inequality constraints are imposed on the product purities (see Eq. (9)):

$$\begin{aligned} Pur_{\mathrm{Ex},k} &= \frac{\int_{t_k}^{t_{k+1}} c_{A,\mathrm{Ex}}(t)\,\mathrm{d}t}{\int_{t_k}^{t_{k+1}} \left[c_{A,\mathrm{Ex}}(t) + c_{B,\mathrm{Ex}}(t)\right]\mathrm{d}t}, \quad Pur_{\mathrm{Ra},k} \\ &= \frac{\int_{t_k}^{t_{k+1}} c_{B,\mathrm{Ra}}(t)\,\mathrm{d}t}{\int_{t_k}^{t_{k+1}} \left[c_{A,\mathrm{Ra}}(t) + c_{B,\mathrm{Ra}}(t)\right]\mathrm{d}t} \end{aligned} \tag{10}$$

and on the internal flow-rate in the first zone:

$$Q_I \leq Q_{\max} \tag{11}$$

The maximal admissible pressure drop in the plant $\Delta p_{\max}$ implies, according to Darcy's law, a certain maximal internal flow-rate in the column:

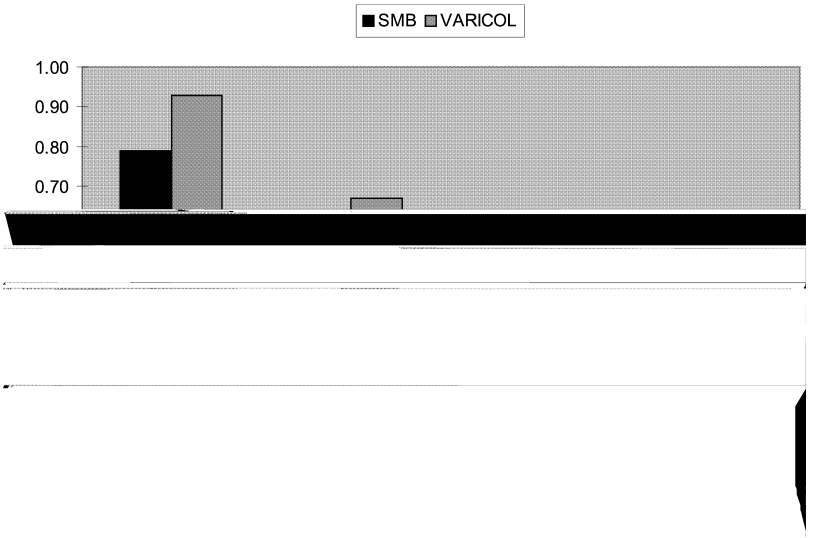

Fig. 8. Comparison of optimized SMB and Vari*col* processes for different number of columns.

converges to a local optimum. In order to check that the obtained results are not likely to be sub-optimal, in each optimization several runs were carried out starting from different initial operating points. For the 6-column Vari*col* case, Fig. 9 shows the evolution of the operating points during the iterative optimization procedure for two different runs. Even for very different initial conditions, the optimizer converged towards the same point. We therefore assume that this point is a global optimum. All iterations presented in Fig. 9 yield feasible points, since we are using a feasible path optimizer. In contrast to a classical SQP-optimizer like E04UCF from the NAG Library, FFSQP checks the feasibility of the solution and stops the line search when an infeasible point is reached. This can be less efficient for oddly shaped feasible regions, but on the other hand for the problem at hand FFSQP is more robust than E04UCF.

The use of FFSQP is also advantageous for analysis purposes, since as a result of an optimization run we obtain a set of feasible points. In Fig. 10, all these feasible points, which were obtained during the optimization of a 6-column Vari*col* process, were plotted in the (m_2–m_3) space. According to the equilibrium theory [4], only the triangular shaped region is the region of complete separation for the true moving bed (TMB) process. Fig. 10 shows that the Vari*col* process is not equivalent to the TMB (whereas SMB is known to be equivalent for sufficiently many columns). The triangle theory here completely fails to predict the optimal operating conditions. This is mainly due to the fact that in the Vari*col* process, the discrete switching dynamics have a stronger effect on the region of complete separation. Therefore more rigorous models (i.e. models which incorporate the discrete switching) have to be used for the design of the Vari*col* process.

From the optimization results given in Tables 2 and 3, it can be concluded that the optimal β_2, β_3-values in SMB and Vari*col* are approximately equal, and in both cases are greater than 1.0. The zones II and III are much longer in the Vari*col* process than in SMB, which enables the higher feed throughput observed in the Vari*col* case. Finally the β_1, β_4-variables, which directly influence the flow-rates in zones I and IV, seem to be adopted in the way that the zones I and IV fulfill their functions (i.e. regeneration of the adsorbent in zone I and recycling of the eluent in zone IV).

6. Conclusions

The rigorous optimization presented here for the SMB and the Vari*col* process clearly shows that a higher production can be achieved with the Vari*col* process compared to SMB. The benefit of the more

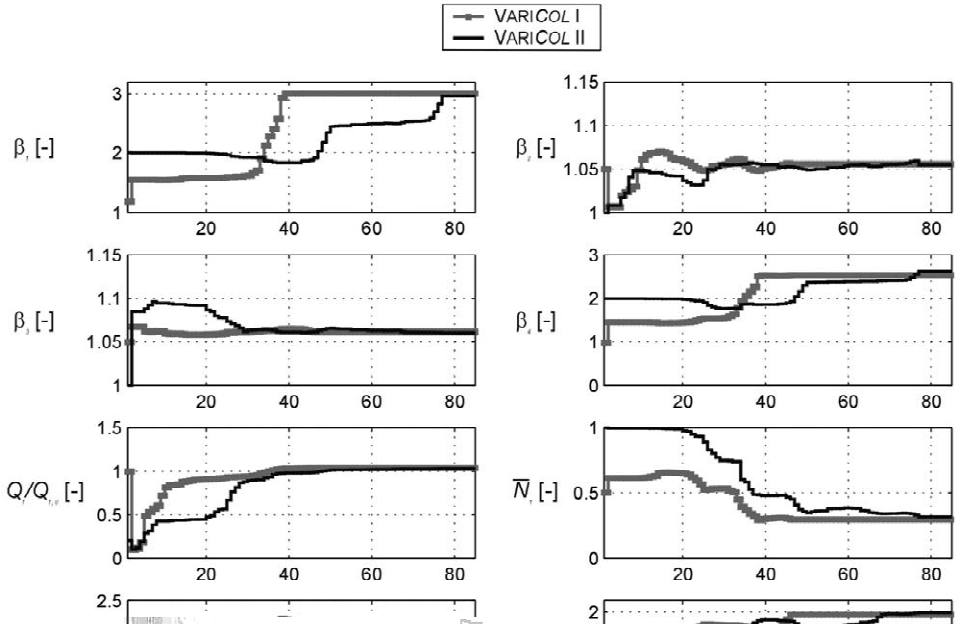

Fig. 9. FFSQP-optimization runs for the 6-column Vari*col* process starting with different initial conditions.

flexible switching strategy of Vari*col* becomes more pronounced for fewer columns. In this work, we reported an optimization strategy to compare SMB and Vari*col* in a systematic and fair manner and applied it to the separation of a mixture of propranolol isomers with strongly nonlinear isotherms. Due to the more flexible use of the solid phase, the Vari*col* process needs one column less than SMB for the same separation task. We showed that the equilibrium theory used in SMB fails to predict the separation behavior of the Vari*col* process. Thus a rigorous optimization strategy has to be used for an optimal design of the novel Vari*col* process.

As discussed above, due to the high sensitivity of the optimal operating points to the model parameters and to process disturbances, feedback control is needed to maintain the desired product purities. The optimization strategy reported in this work can act as a setpoint generator for a low-level controller. The development and design of such a controller which may use the sub-intervals as compensation variables is one important subject of our future research.

7. Nomenclature

c_i (g/ml)	concentration of component i in the bulk phase
c_{pi} (g/ml)	concentration of component i in the particle phase
$c_{\mathrm{ax},k}$ (g/ml)	internal axial concentration profile
D_{ax} (cm^2/s)	axial dispersion coefficient
$D_{p,i}$ (cm^2/s)	particle dispersion of component i
H (cm)	height equivalent to a theoretical plate

u (cm/s)	interstitial velocity
x (cm)	axial coordinate
V_S (m^3)	volume of the solid phase
Greek letters	
Φ (–)	operator representing the dynamical behavior from period to period
β_i (–)	transformed degrees of freedom, $i = 1, \ldots, 4$
λ_i (–)	linear term of the modified Langmuir isotherm, $i = 1, 2$
δt_z (–)	sub-switching times, $z = 1, \ldots, 4$
ε_b (–)	porosity of the bulk phase
ε_p (–)	porosity of the particle phase
ε^* (–)	total porosity of the bed
τ (s)	period
Subscripts	
i	component $i = 1, 2$
j	product $j = 1, 2$
z	zones of the process $z = 1, \ldots, 4$
De	desorbens
Ex	extract
Fe	feed
Ra	raffinate
S	solid phase
SMB	simulated moving bed process
TMB	true moving bed process
Vari*col*	variable column length process
I, II, III, IV	zones of the SMB or Vari*col* process

Acknowledgements

The authors are indebted to P. Adam and F. Guende (NovaSep, Pompey) for their support and valuable input to this work. The financial support of the Deutsche Forschungsgemeinschaft, in the context of the research cluster ''Integrated Reaction and Separation Processes'' at the University of Dortmund (Schm 808/5-1) under grant (DFG En 152/26) is very gratefully acknowledged.

Appendix A

Parameters of the propranolol isomers mixture

Symbol	Value (units)		Signification
L	10.0 (cm)		Column length
D	1.0 (cm)		Column diameter
ε_b	0.4		Bulk void porosity
ε_p	0.5		Particle void porosity
ε^*	0.7		Total porosity $\varepsilon^* = \varepsilon_b + (1 - \varepsilon_b)\varepsilon_p$
$c_{\mathrm{Fe},i}$	7.5+7.5 (g/l)		Feed concentrations
d_p	20 (μm)		Particle diameter
$D_{p,i}$	$1.0 \cdot 10^{-5}$ (cm^2/s)		Particle diffusion coefficient
$D_{\mathrm{ax},i}$	$1.0 \cdot 10^{-6}$ (cm^2/s)		Axial diffusion coefficient of the bulk phase
	Sp. A	Sp. B	
$k_{\mathrm{eff},i}$	$0.56 \cdot 10^{-2}$	$0.33 \cdot 10^{-2}$	Mass transfer resistance
	Sp. A	Sp. B	Extended biLangmuir isotherm
λ_i	2.68	2.2	$q_i = \lambda_i C_{p,i} + \frac{N k_i C_{p,i}}{1 + k_1 C_{p,1} + k_2 C_{p,2}}$
NK_i	0.9412	0.4153	
K_i	0.340	0.262	
H_i	2.04	1.647	
k_0	0.033		Darcy's law: proportional factor k_0 and the maximal attainable pressure drop over a chromatographic column
$\Delta p_{\max}$	20 (bar)		
A	$4 \cdot 10^{-4}$ (cm)		Height equivalent to theoretical plate $H = A + B\,u$
B	0.25735 (s)		

References

[1] H. Colin, O. Ludemann-Hombourger, R.M. Nicoud, Pharma. Visions (2001) 26.
[2] M. Schulte, J.N. Kinkel, R.M. Nicoud, F. Charton, Chem. Ing. Tech. 68 (1996) 670.
[3] M. Juza, M. Mazzotti, M. Morbidelli, Trends Biotechnol. 18 (2000) 108.
[4] J. Bléhaut, R.M. Nicoud, Analusis Mag. 26 (7) (1998) 60.
[5] G. Biressi, F. Quattrini, M. Juza, M. Mazzotti, V. Schurig, M. Morbidelli, Chem. Eng. Sci. 55 (2000) 4537.
[6] O. Di Giovanni, M. Mazzotti, M. Morbidelli, F. Denet, W. Hauck, R.M. Nicoud, J. Chromatogr. A 919 (1) (2001) 1.
[7] G. Hotier, R.M. Nicoud, M. Perrut, French Pat. 9301703 (1993).
[8] A. Depta, T. Giese, M. Johannsen, G. Brunner, J. Chromatogr. A 865 (1999) 175.
[9] P. Adam, R.M. Nicoud, M. Bailly, O. Ludemann-Hombourger, US Pat. 6 136 198 (2000).
[10] O. Ludemann-Homburger, R.M. Nicoud, M. Bailly, Sep. Sci. Technol. 35 (12) (2000) 1829.
[11] A. Toumi, F. Hanisch, S. Engell, Ind. Eng. Chem. Res. 41 (2002) 4328.
[12] A. Toumi, S. Engell, F. Hanisch, Chem. Ing. Tech. 10 (2002) 1483.
[13] O. Ludemann-Homburger, G. Pigorini, R.M. Nicoud, D.S. Ross, G. Terfloth, J. Chromatogr. A 947 (1) (2002) 56.
[14] D.B. Broughton, US Pat. 2 985 589 (1961).
[15] D.B. Broughton, US Pat. 3 291 726 (1966).
[16] D.M. Boyd, C. Hills, US Pat. 3 268 605 (1966).
[17] D.M. Boyd, US Pat. 3 266 604 (1966).
[18] F. Charton, R.M. Nicoud, J. Chromatogr. A 702 (1995) 97.
[19] G. Hotier, R.M. Nicoud, US Pat. 5 578 215 (1996).
[20] T. Gu, Mathematical Modelling and Scale up of Liquid Chromatography, Springer, New York, 1995.
[21] G. Ganetsos, P.M. Barker, Preparative and Production Scale Chromatography, Marcel Dekker, New York, 1993.
[22] G. Guiochon, S.G. Golshan-Shirazi, A.M. Katti, Fundamentals of Preparative and Nonlinear Chromatography, Academic Press, Boston, 1994.
[23] D. Ruthven, C. Ching, Chem. Eng. Sci. 44 (1989) 1011.
[24] G. Dünnebier, J. Fricke, K.-U. Klatt, Ind. Eng. Chem. Res. 39 (2000) 2290.
[25] K.-U. Klatt, G. Dünnebier, S. Engell, F. Hanisch, Computers Chem. Eng. 24 (2000) 1119.
[26] G. Dünnebier, Dissertation, Department of Chemical Engineering, University of Dortmund, 2000 Shaker-Verlag, Aachen, 2000.
[27] P.N. Brown, G.D. Byrne, A.C. Hindmarsh, Siam J. Sci. Comput. 10 (1989) 1038.
[28] S. Karlsson, F. Petterson, H. Skrifvars, T. Westerlund, S. Pierucci (Eds.), European Symposium on Computer Aided Process Engineering ESCAPE-10, 2000, p. 463.
[29] G. Biressi, O. Ludemann-Hombourger, M. Mazzotti, R.M. Nicoud, M. Morbidelli, J. Chromatogr. A 976 (2000) 3.
[30] M. Mazzotti, G. Storti, M. Morbidelli, J. Chromatogr. A 769 (1997) 3.
[31] J.L. Zhou, A.L. Tits, C.T. Lawrence, Users's Guide for FFSQP version 3.7, Electrical Engineering Department, University of Maryland, 1997.
[32] R.M. Nicoud, A. Seidel-Morgenstern, Isolation Purif. 2 (1996) 165.
[33] The NAG Fortran Library. Mark 15, Vols. 1–10, NAG Ltd, Oxford, 1991.